Supporting information

A composite dielectric membrane with low dielectric loss for dendrite-free lithium deposition in lithium metal batteries

*Zetao Ren, [#a] Sichen Gu, [#*b] Tong Li, [a] Linkai Peng, [a] Changhong Zou, [a] Feiyu Kang *[a] and Wei Lv *[a]*

Z. Ren, T. Li, L. Peng, F. Kang, W. Lv

Shenzhen Geim Graphene Center, Shenzhen Key Laboratory for Graphene-based Materials, Tsinghua Shenzhen International Graduate School, Tsinghua University, Shenzhen, 518055, China

E-mail: lv.wei@sz.tsinghua.edu.cn; fykang@sz.tsinghua.edu.cn

S. Gu

Laboratory for Advanced Materials and Batteries, Department of Material Science, Shenzhen MSU-BIT University, Shenzhen, 518172, China

E-mail: sichen.gu@smbu.edu.cn

Keywords: Lithium Metal batteries, Dielectric Constant, Dielectric loss, Porous Structure.

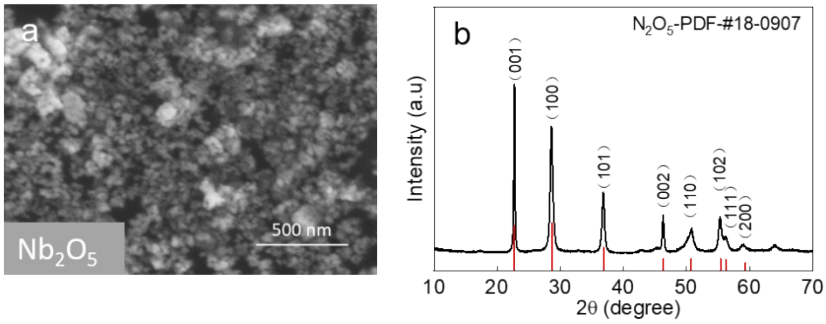

Figure S1. a) SEM morphology of Nb_2O_5, and b) XRD pattern of Nb_2O_5.

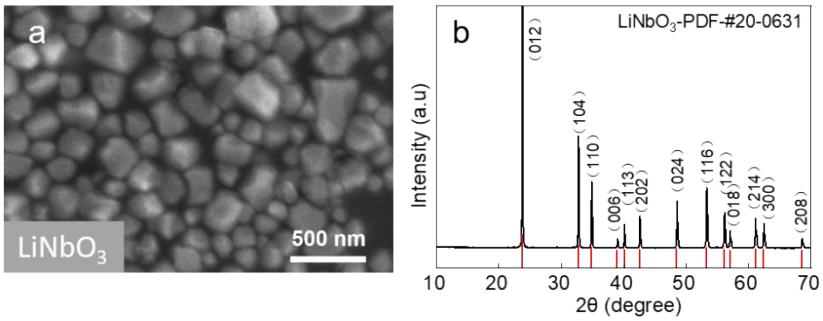

Figure S2. a) SEM morphology of $LiNbO_3$, and b) XRD pattern of $LiNbO_3$.

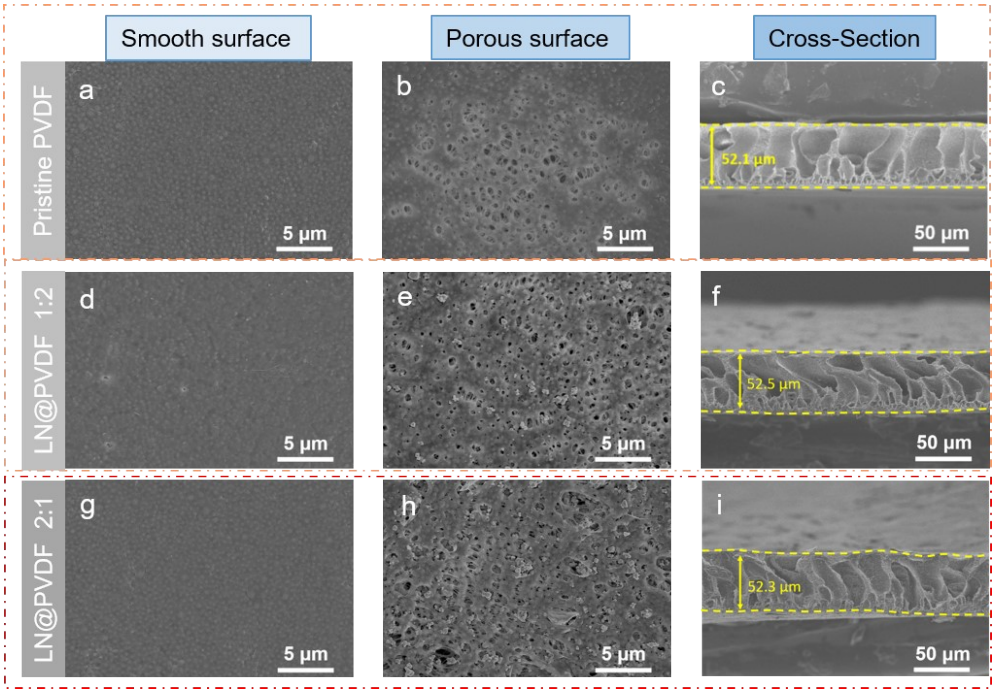

Figure S3. The smooth surface, porous surface and cross-sectional SEM morphologies of the (a-c) porous PVDF, (d-f) LN@PVDF 1:2, and (g-i) LN@PVDF 2:1.

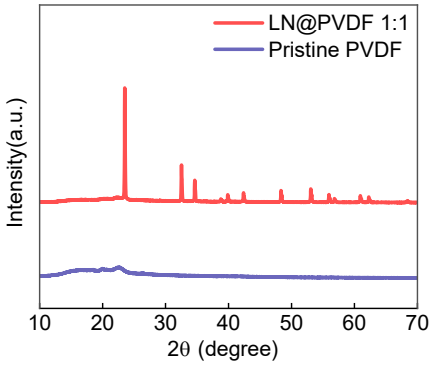

Figure S4. XRD patterns of pristine PVDF and LN@PVDF 1:1.

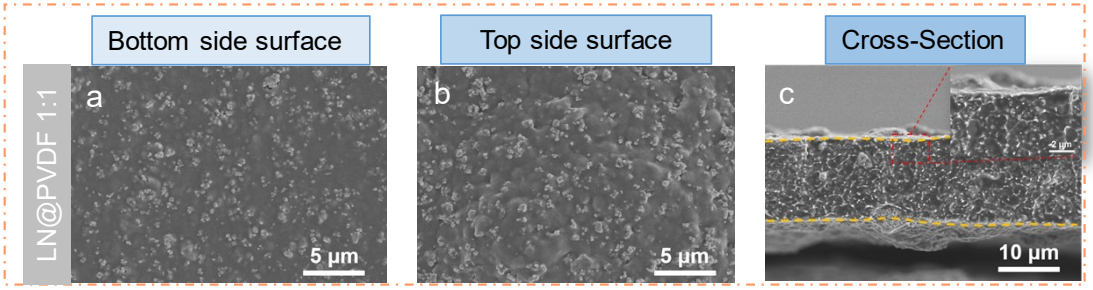

Figure S5. SEM images of the LN@PVDF-np 1:1.

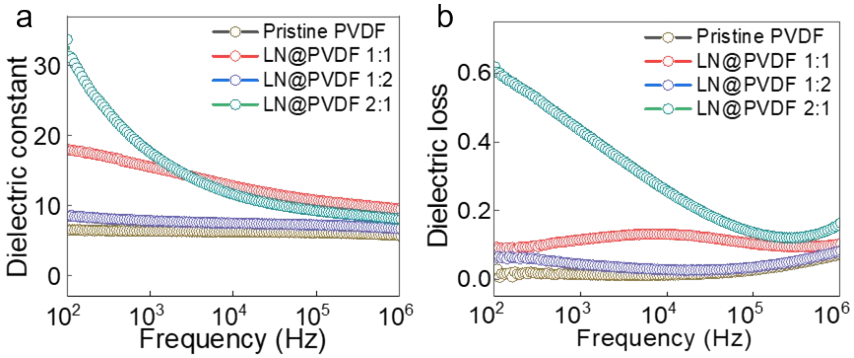

Figure S6. a) Dielectric constant, and b) dielectric loss of the pristine PVDF, LN@PVDF 1:1, LN@PVDF 1:2, and LN@PVDF 2:1.

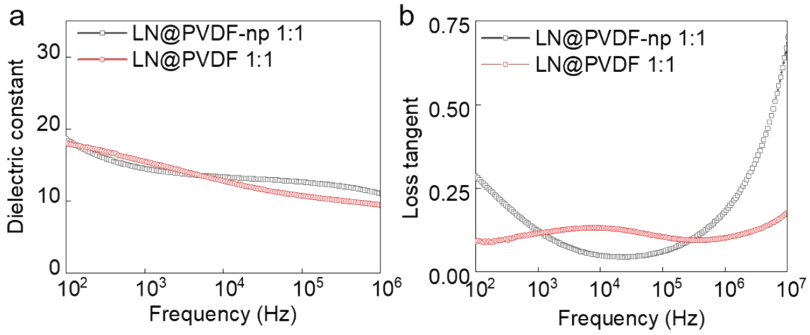

Figure S7. a) The Dielectric constant diagram, and b) dielectric loss of the LN@PVDF 1:1 and LN@PVDF-np 1:1 film.

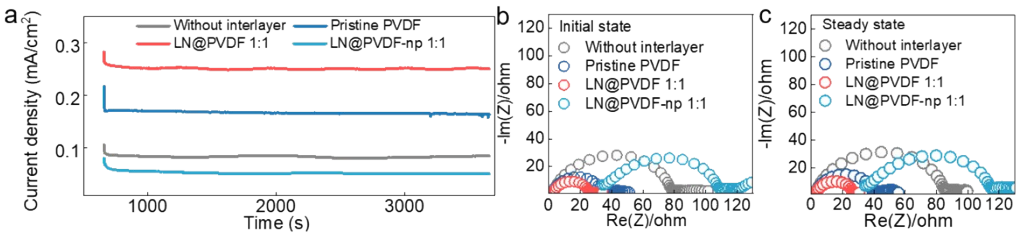

Figure S8. The Li-ion transference number (t_{Li+}) measurement using the Li-Cu cells with PVDF, LN@PVDF 1:1, LN@PVDF-np 1:1 and without interlayer. a) Steady-state current measurement, b,c) impedance spectra for the initial state and steady-state.

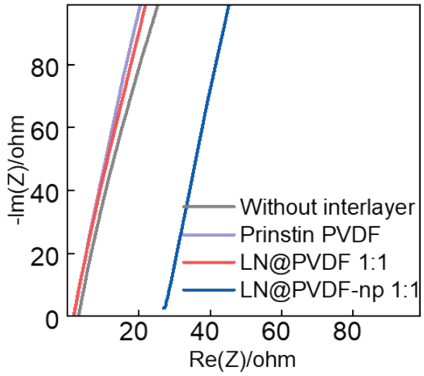

Figure S9. The ion conductivity measurement for different samples.

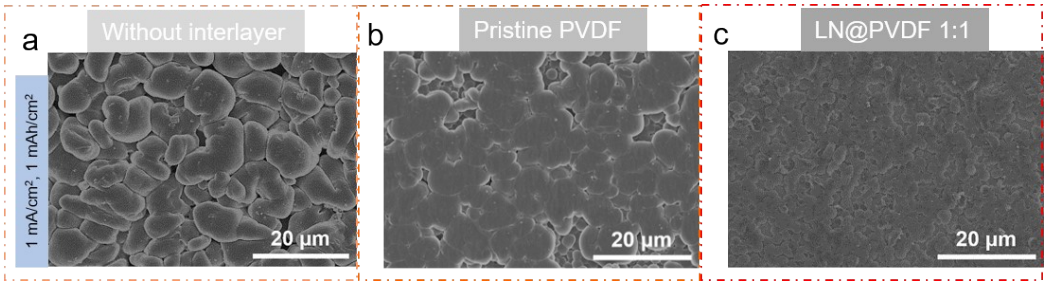

Figure S10. SEM images after Li deposition for 1 mAh cm^{-2} a) without interlayer, b) with pristine PVDF, and c) with LN@PVDF 1:1 respectively.

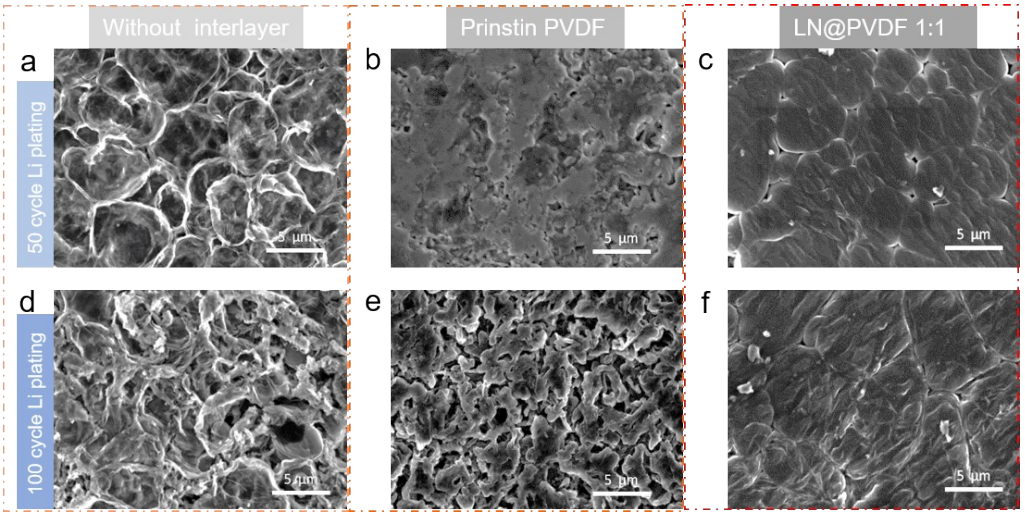

Figure S11. a-c) SEM images of the deposited Li on the Cu after the 50th plating without interlayer, with the interlayer of PVDF film, and LN@PVDF 1:1. d-e) SEM images of the deposited Li on the Cu after the 100th plating without interlayer, with the interlayer of PVDF film, and LN@PVDF 1:1.

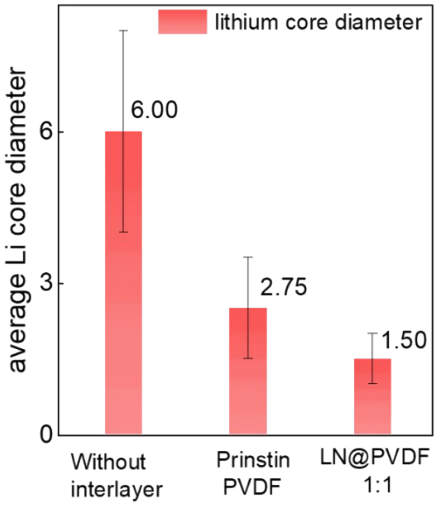

Figure S12. Statistical measurement for the lithium nuclei diameter under the current density of 1 mA cm^{-2} and the capacity of 0.5 mAh cm^{-2}

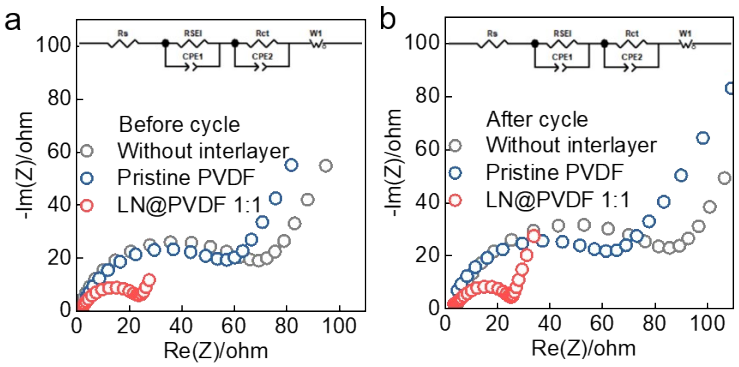

Figure S13. AC impedance spectra of Li-Cu half-cell with PVDF, LN@PVDF 1:1 and without interlayer before and after the 50 times plating and stripping. a) The impedances of the half-cells before cycling with PVDF, LN@PVDF 1:1 and without interlayer are 58, 23, and 67 Ω respectively; b) The impedances of the half-cells after cycling with PVDF, LN@PVDF 1:1 and without interlayer are 61, 24, and 82 Ω, respectively.

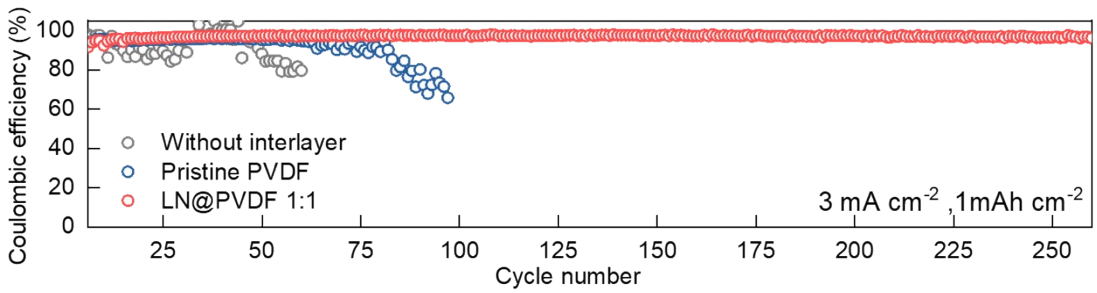

Figure S14. CE of the Li-Cu with the PVDF interlayer, LN@PVDF 1:1 interlayer and without interlayer, under the current density and capacity of 3 mA cm^{-2}, 1 mAh cm^{-2}.

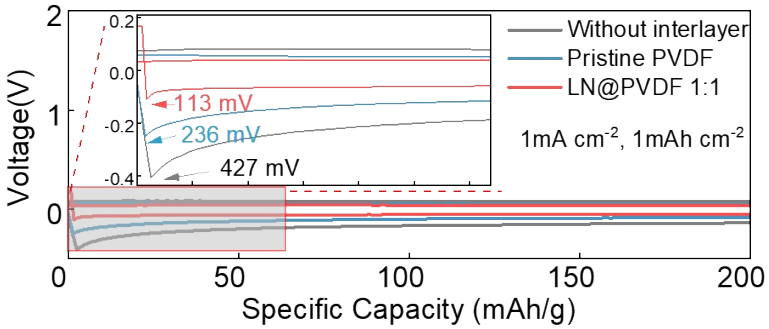

Figure S15. The nucleation overpotentials under the current densities of 1 mA cm^{-2}.

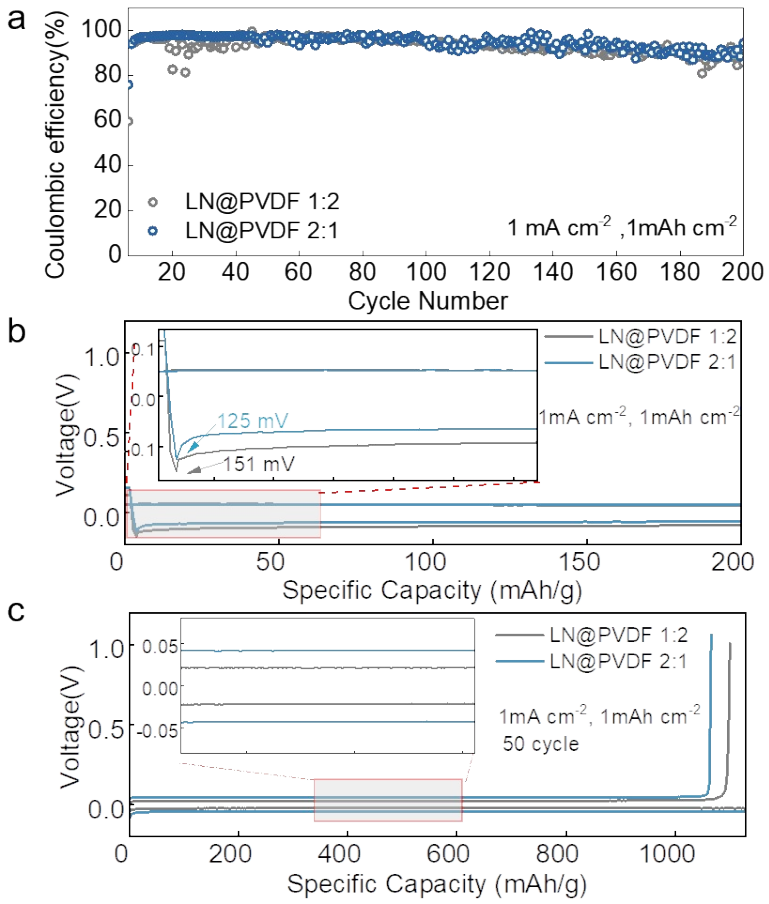

Figure S16. a) CE of Cu-Li cell with LN@PVDF 1:2 and LN@PVDF 2:1, b) The nucleation overpotentials of the first cycle under the current densities of 1 mA cm^{-2}, c) the 50th plating and stripping curves under the current density of 1 mA cm^{-2}.

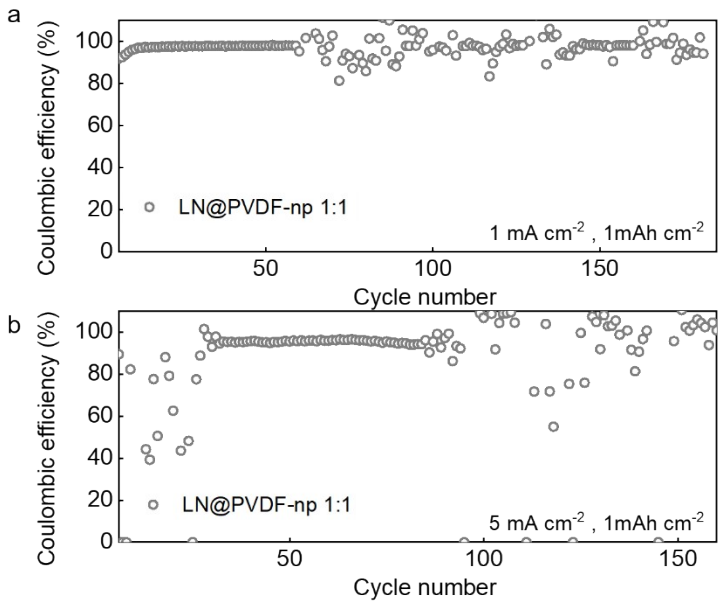

Figure S17. CE of Li-Cu half-cell with LN@PVDF-np 1:1 (1 mA cm^{-2}, 1 mAh cm^{-2}; 5 mA cm^{-2}, 1 mAh cm^{-2}).

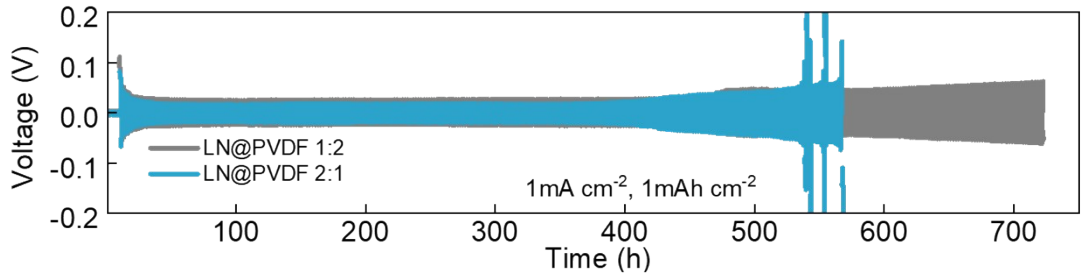

Figure S18. The time-voltage curves of Li-Li symmetric cells with LN@PVDF 1:2 and LN@PVDF 2:1.

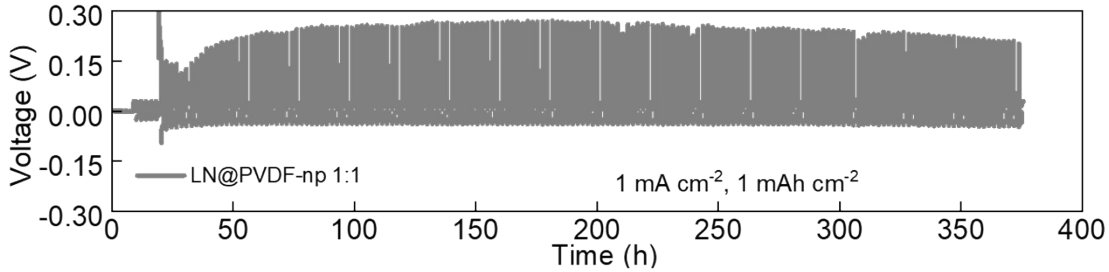

Figure S19. The time-voltage curve of the Li-Li symmetric cell with the LN@PVDF-np 1:1.

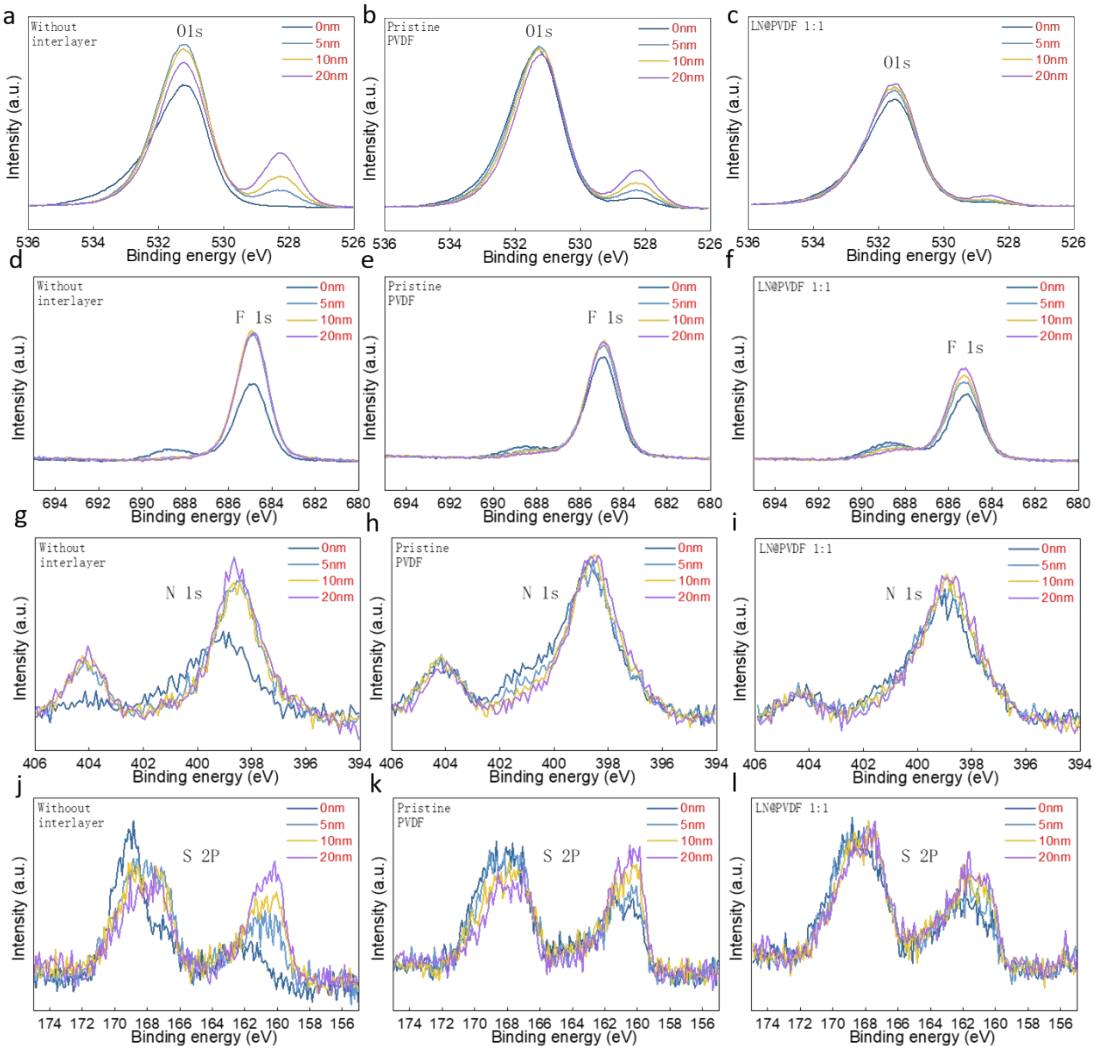

Figure S20. O *1s*, F *1s*， N *1s* and S *2p* spectra of the SEI on lithium electrodes at different depths.

Table S1. The fitted R_{SEI} and R_{ct} values of cells in Figure 4e

Before cycle	**R_{SEI}**	**R_{ct}**
Without interlayer	55	17.3
Pristine PVDF	46.8	15.4
LN@PVDF 1:1	26.5	13

Table S2. The fitted R_{SEI} and R_{ct} values of cells in Figure 4f

After cycle	**R_{SEI}**	**R_{ct}**
Without interlayer	63.9	13

Pristine PVDF	51.7	12
LN@PVDF 1:1	27.3	9.3

Table S3. The fitted R_{SEI} and R_{ct} values of cells in Figure 4g

After cycle	**R_{SEI}**	**R_{ct}**
LN@PVDF 1:2	40.3	14.3
LN@PVDF 2:1	32.6	12.3
LN@PVDF 1:1	29.1	10.8

Table S4. The fitted R_{SEI} and R_{ct} values of cells in Figure 5f

After cycle	**R_{SEI}**	**R_{ct}**
Without interlayer	93.36	982
Pristine PVDF	63.3	633
LN@PVDF 1:1	51.5	313